Supplementary Information for "Drivers of Antarctic sea ice advance”

Kenza Himmich[1]
Martin Vancoppenolle[1]
Gurvan Madec[1]
Jean-Baptiste Sallée[1]
Paul R. Holland[3]
Marion Lebrun[2,1]

[1] Sorbonne Université, Laboratoire d’Océanographie et du Climat, CNRS/IRD/MNHN, Paris, France
[2] Takuvik, Université de Laval, Québec QC, Canada
[3] British Antarctic Survey, Natural Environment Research Council, Cambridge, UK
[4] Université Grenoble Alpes, Inria, CNRS, Grenoble INP, LJK, 38000 Grenoble, France

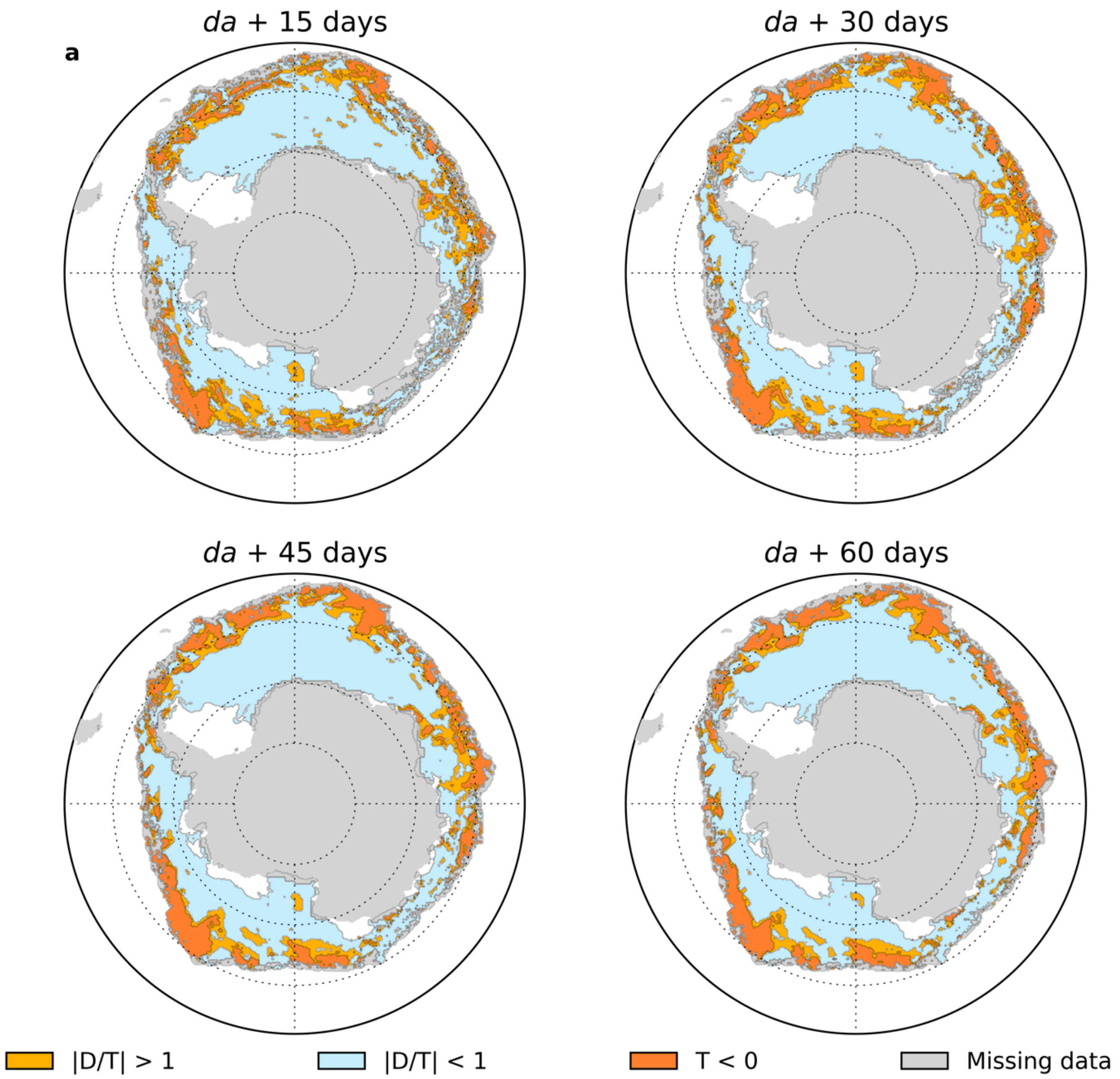

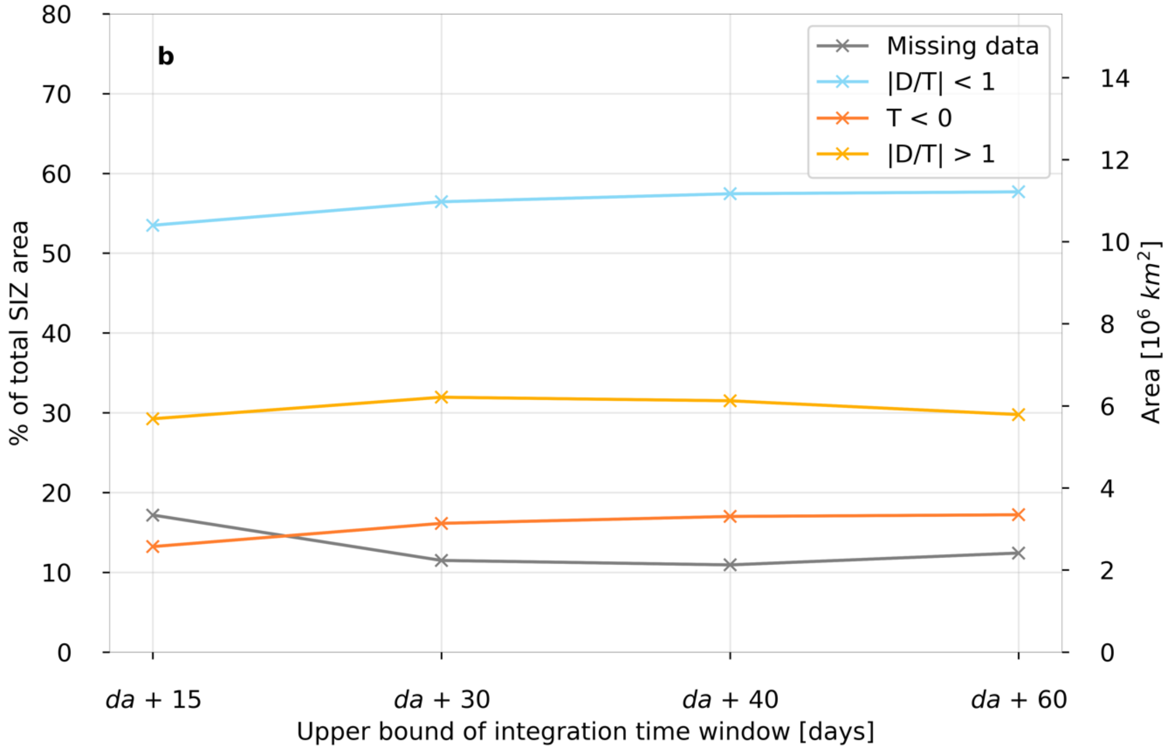

Fig. S1 **Sensitivity of the SIC-budget-based regions to the size of the time-integration window. a** shows the sensitivity of the borders of four regions with characteristic SIC-budget: melting (T < 0; in orange), dominant dynamics (D/T > 1; yellow and orange regions), dominant thermodynamics (D/T < 1; in blue) and missing data (in grey). **b** shows the fractional area sensitivity of the same four regions. White patches in **a** indicate regions out of the seasonal ice zone.

The SIC budget at the date of advance has large uncertainties, hence we integrate in time over a time window spanning part of the sea ice season. Here we find that the SIC budget-derived limit between the *inner* and *outer* zones weakly depends on the size of the time integration window, suggesting it is a robust feature. We estimate an uncertainty on the size of the *outer zone* of 3% of the SIZ area. We define this uncertainty as the difference between the maximum area and the minimum area that the *outer zone* can reach according to the time window.

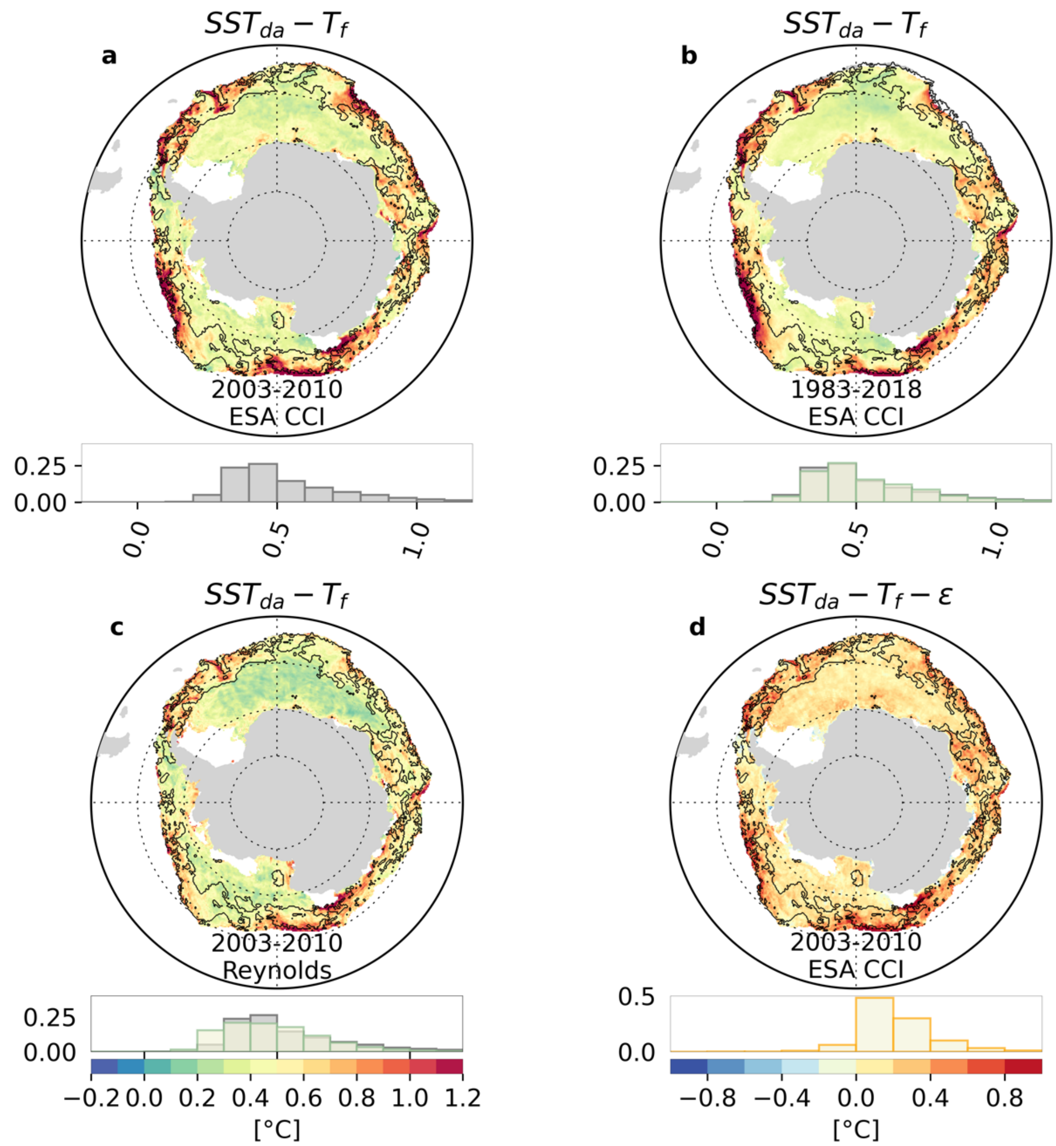

Fig. S2 **Robustness of the *inner-outer zone* limit across time periods, SST products and uncertainty.** SST at the date of advance referenced to freezing temperature (T_f, assumed constant at -1.8°C), based on **a** ESA CCI SST, averaged over 2003-2010 **b** ESA CCI SST, averaged over 1983-2018 **c** Reynolds' SST, averaged over 2003-2010. **d** Difference between the SST at the date of advance referenced to freezing temperature (SST_{da} - T_f) and the uncertainty (ε) on the ESA CCI SST analysis, averaged over 2003-2010. Corresponding frequency histograms are shown under each map in grey (**a**) or beige (**b**, **c**, **d**). In **b** and **c**, the grey histogram is the same as in **a** and used as a reference distribution. The black contour defines the limit between the *inner* and *outer zones*. White patches indicate regions out of the seasonal ice zone.

SST at date of advance slightly differs according to the averaging period (2003-2010 or 1983-2018) or the product (ESA CCI or Reynolds'), however the effect of the *inner-outer zone* limit is always visible. Hence, the *inner-outer zone* limit is robust. (SST_{da} - T_f) is predominantly higher than uncertainty, even more so in the *outer zone*. This is consistent with a higher SST_{da} in the *outer zone* compared to the *inner zone*. In the *inner zone*, higher than uncertainty (SST_{da} - T_f) could be due to a spatial averaging effect: a 15% ice covered grid point is not necessarily at the freezing point everywhere.

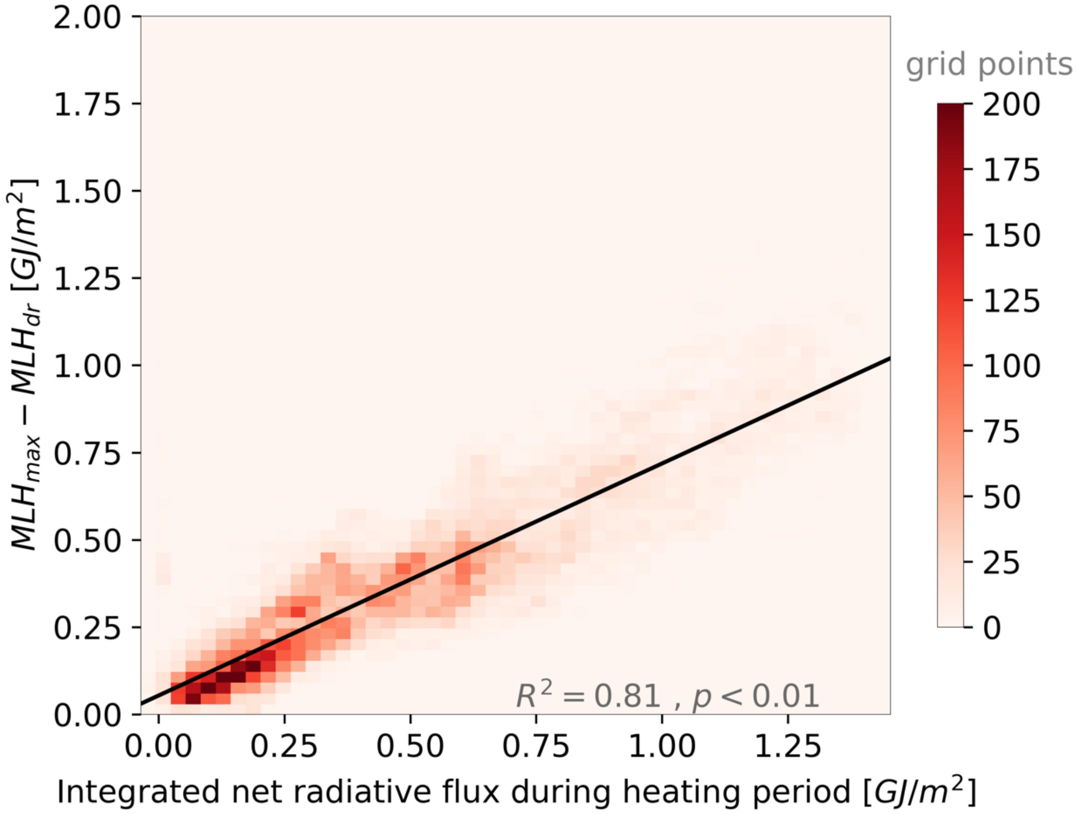

Fig. S3 **Spatial relationship between the seasonal increase of MLH and the total surface radiative heating over the ocean heating period, from the date of retreat to the date of seasonal maximum MLH.** Climatological MLH derived from thermal infra-red radiance satellite SST (ESA CCI) and a climatology of MLD (1979-2018); observed climatological net radiative flux obtained from ISCCP (1984-2016). The relationship is represented as a 2D histogram showing only grid points from the *inner zone*. Color gives the number of points in each pixel of the 2D histogram space. A Least Square linear regression was performed and the corresponding regression line, R^2 and p-values are shown.

The seasonal maximum MLH is tightly linked to the date of sea ice retreat (see Figure 3c). Here we show that this link is due to a strong control of the maximum MLH by the net radiative flux absorbed by the ocean, which itself constrained by the date of sea ice retreat.

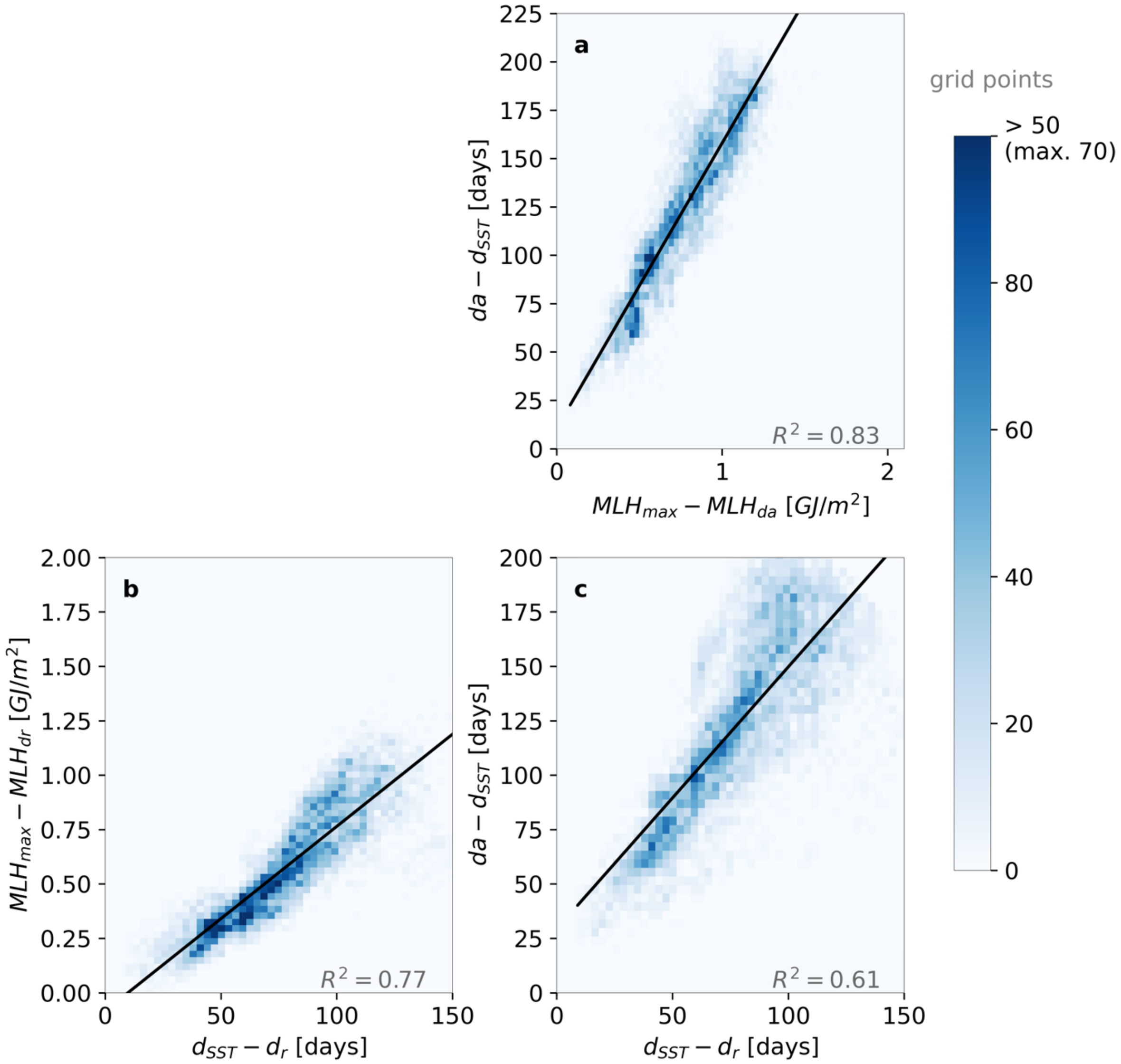

Fig. S4 **Selected *outer zone* spatial relationships between the 1983-2018 climatological maps of key variables displayed in Fig. 1, plotted as 2D histograms.** **a**, *da* vs MLH_{max}, **b**, MLH_{max} vs *dr* and **c**, *da* vs *dr*. Anomalies are used, tailored to best showcase the relevant relationships (see Methods). *da* (*dr*) anomalies refer to the date of maximum SST (d_{SST}) such that positive anomalies indicate later advance (retreat). In **a** (**b**), MLH_{max} anomalies refer to the MLH value at sea ice advance (retreat) date, which is close to but not exactly zero, because the SST is a few tenths of degree above freezing (see Fig. S2). Only grid points from the *outer zone* are shown. Color gives the number of points in each pixel of the 2D histogram space. A Least Square linear regression was performed for each plot; the corresponding regression line (significant at 99%), and corresponding R^2 are given.

The *dr*-MLH_{max}-*da* linear relationships are strong in the *inner zone.* Here, we show that these relationships are significantly weaker in the *outer zone*, according to Fisher's Z-test at a 0.01 significance level. The *dr*-*da* relation is the weakest. By contrast, the MLH_{max}-*da* relation, still explains a large part (83%) of the variance in the climatological date of advance.

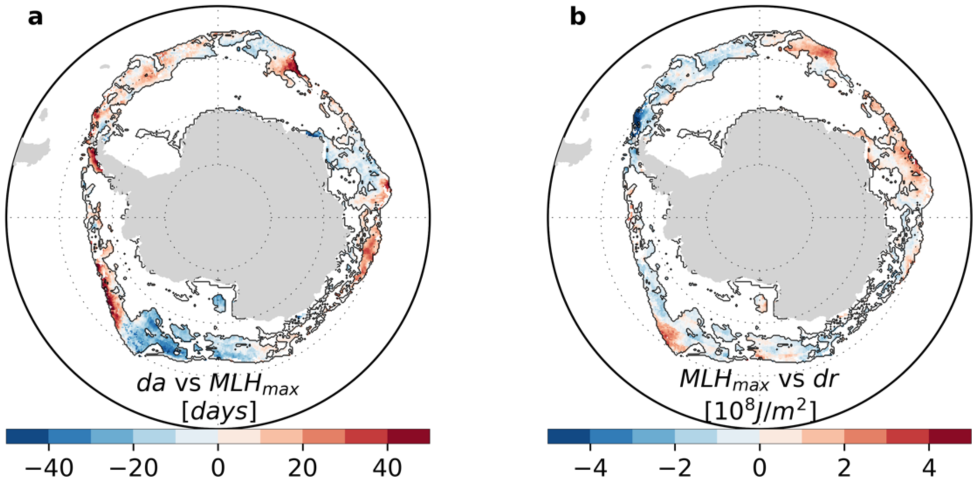

Fig. S5 **Spatial distribution of errors on the *dr-MLH_{max}-da* linear regressions, in the *outer zone*.** Error are defined as the residuals of **a**, the *da* vs *MLH_{max}* and **b**, the *MLH_{max}* vs *dr* linear regressions (Fig. S4). Residuals are calculated as the difference between the actual value of a given grid point and the predicted value based on the model fit. Only grid points located in the *outer zone* are displayed.

In the *outer zone*, the *dr-da* relation is weaker than the *dr-MLH_{max}* and the *MLH_{max} -da* relations. Here we show that this is might be due to different spatial distributions of the errors on the *dr-MLH_{max}* and the *MLH_{max} -da* linear regressions.